Predicting ^{13}C NMR Spectra by DFT Calculations

Alessandro Bagno,*,† Federico Rastrelli,† and Giacomo Saielli‡

Dipartimento di Scienze Chimiche, Università di Padova, and Istituto per la Tecnologia delle Membrane del CNR, Sezione di Padova, via Marzolo, 1-35131 Padova, Italy

Received: May 14, 2003; In Final Form: September 22, 2003

^{13}C chemical shifts and $^{n}J_{CH}$ coupling constants have been determined both experimentally (by means of *J*-resolved NMR spectroscopy) and theoretically (by DFT calculations) for a series of organic molecules. With the exception of halogen-bonded carbon nuclei, a good correlation is observed between experimental and calculated data. The magnitude of the most important contributions to the spin−spin coupling constant (Fermi-contact, diamagnetic, and paramagnetic spin−orbit contributions) has been determined. The spin−orbit terms are negligible or cancel out ($^{1}J_{CH}$ and $^{3}J_{CH}$), thus leaving the contact term as the only relevant contribution, but become important for $^{2}J_{CH}$ in aromatic (but not in aliphatic) compounds. Relativistic effects on the ^{13}C chemical shift of carbon bonded to a fairly heavy atom (bromine) have also been investigated. Finally, conformational effects on the long-range $^{n}J_{CH}$ coupling constants has been investigated in a model alkane derivative (*n*-butyl chloride). The implications to structure prediction and determination by NMR are discussed.

Introduction

NMR spectroscopy continues to be the most valuable tool for structure elucidation in solution. By far, the most common nuclei studied in the NMR of organic and bio-organic molecules are ^{1}H and ^{13}C. The wide array of available techniques yields a wealth of information, not only in the form of just chemical shifts and coupling constants of the involved nuclei, but also as through-bond and through-space connectivities between them. Very often, careful application of available pulse sequences results in a consistent determination of C−H connectivities, leading to cogent indication on the molecular structure (often complemented by NOE-derived data to supply conformational information). This is made possible by exploiting heteronuclear *J*-couplings in various 2D sequences such as HSQC, HMQC, HMBC, etc., which, among other things, are tailored to emphasize short- or long-range $^{13}C-^{1}H$ couplings through the judicious selection of a delay time related to $1/(2J_{CH})$, where J_{CH} is an average value expected for the molecule of interest.

A large body of data is available to rationalize the trends between chemical shifts, coupling constants, and molecular structure.[1] However, establishing precise relationships requires the evaluation of many local factors, notably long-range complex substituent effects on chemical shifts and conformational effects on coupling constants. An a priori knowledge of these fundamental NMR parameters would, therefore, be highly desirable since it would allow the major features of 2D heterocorrelated spectra to be predicted and, eventually, lead to precious structural information. This particularly holds for atypical situations which cannot be treated through a comparison with known data, e.g. when steric or strain effects, or uncommon atoms, are present.

The general problem of calculating nuclear shieldings, including those of ^{13}C, recently has been reviewed and poses no special problem, at least in simple molecules containing light atoms.[2] Indeed, such calculations by means of correlated methods (both ab initio and DFT) are abundant in the literature, and no attempt will be made to report on them other than citing a few recent interesting trends, e.g. using computed chemical shifts to probe noncovalent interactions[3] and shielding tensor properties[4] and to determine the structure of naturally occurring molecules.[5] Empirical corrections to calculated shifts were also investigated.[6]

Conversely, even though computational studies of spin−spin couplings are flourishing,[2] notably in relation to the recent research on through-hydrogen-bond and through-space couplings,[7,8] much less is known about $^{13}C-^{1}H$ couplings. In particular, the relative contribution of the contact and spin−orbit terms to J_{CH} couplings has been established only for relatively few molecules.[9−12] In this regard, one should remark that $^{13}C-^{1}H$ (and $^{13}C-^{13}C$) couplings are important in establishing conformational issues, especially of carbohydrates and related species, and such calculations are correspondingly being intensively carried out.[9,13−15]

We have previously shown the reliability of DFT calculations as a tool to predict ^{1}H NMR spectral parameters in a variety of organic molecules.[16,17] Thus, it was shown that (a) B3LYP/cc-pVTZ//B3LYP/6-31G(d,p) calculations allow ^{1}H chemical shifts to be predicted to a good accuracy and (b) J_{HH} couplings can be reliably obtained from the calculation of the Fermi-contact term at the same level, because it is the only relevant contribution since the two spin−orbit coupling terms cancel out despite their substantial magnitude.

We should recall at this point an inherent limitation of DFT methods: as has been thoroughly emphasized,[2] there is no systematic or consistent way to improve the accuracy of the results thus obtained, in contrast to ab initio methods. However (as will become apparent from our results), DFT methods are the only ones that can be applied, at a reasonable computational cost, to sufficiently complex molecular systems as to pose challenging issues to the experimental NMR spectroscopist, i.e.,

* Address correspondence to this author. Phone: +39 0498275295. Fax: +39 0498275239. E-mail: alessandro.bagno@unipd.it.
† Dipartimento di Scienze Chimiche, Università di Padova.
‡ Istituto per la Tecnologia delle Membrane del CNR, Sezione di Padova.

10.1021/jp0353284 CCC: $25.00
Published on Web 10/25/2003

CHART 1: Compounds Used in the Calculation of ^{13}C NMR Parameters[a]

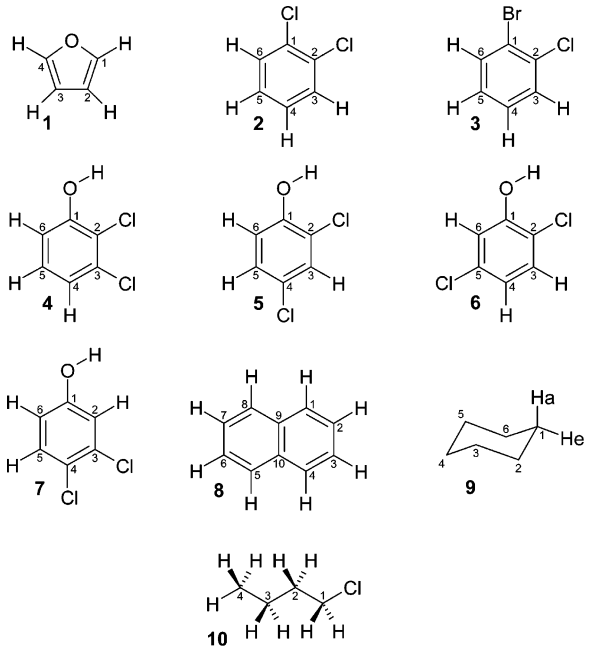

[a] Numerical labels refer to carbon atoms and the corresponding attached hydrogen atoms.

to cases where computational chemistry can be expected to play a decisive role.

Hence, following the same approach, in the present work we focus our attention on NMR spectral parameters of ^{13}C in small organic molecules, partly chosen among those of ref 16, i.e., furan, *o*-dichlorobenzene, *o*-bromochlorobenzene, 2,3-, 2,4-, 2,5-, and 3,4-dichlorophenol, naphthalene, cyclohexane, and *n*-butyl chloride (Chart 1). This selection offers the opportunity to test a variety of ^{13}C chemical shifts and couplings in common environments, including some cases where carbon is bonded to fairly heavy atoms (Cl, Br). These are expected to provide information on the importance of relativistic effects on ^{13}C parameters, which are well-known and understood when carbon is bonded to several heavier atoms such as iodine.[18]

Experimental and Computational Section

All molecules investigated are commercial and were used as received. NMR measurements were carried out at 298 K on Bruker Avance DMX 600 and DRX 300 spectrometers, equipped with a 5-mm TXI (^{1}H, ^{13}C, ^{15}N) *xyz*-gradient inverse probe and a 5-mm BBO *z*-gradient reverse probe, respectively. Heteronuclear *J*-resolved spectra were acquired by using standard spin-flip and gated-decoupling sequences, with broad-band ^{1}H preirradiation for NOE enhancement.[19] Where needed, the spin-flip sequence was made selective by replacing the hard ^{1}H π pulse with a BURP shaped pulse.[20]

The calculations of the chemical shift and spin−spin coupling constants for the model systems have been performed following ref 16. Thus, geometries were optimized by DFT with the B3LYP hybrid functional[21] and the 6-31G(d,p) basis set with use of Gaussian 98.[22] Geometries were optimized with no use of symmetry; however, the resulting structures belonged to the nominal symmetry group within a tolerance of $10^{-5}-10^{-4}$ Å. Nuclear shieldings were computed at two levels of theory: employing the Perdew 86[23] exchange-correlation functional and the IGLO-III basis set[24] (PW86/IGLO-III) as implemented in the program DeMon-NMR,[25] and at the B3LYP/cc-pVTZ level,[21,26] with Gaussian 98. The ^{13}C chemical shift is obtained as $\delta = \sigma_{ref} - \sigma$, where σ_{ref} is the shielding constant of ^{13}C in tetramethylsilane and σ is the same parameter in the molecule of interest. Spin−spin coupling is recognized as arising from the sum of three main contributions, namely the Fermi Contact (FC), Diamagnetic Spin−Orbit (DSO), and Paramagnetic Spin−Orbit (PSO), while the Spin−Dipole (SD) term is generally negligible for these nuclei.[2] Therefore, the total value of *J* is expressed as $J = J^{FC} + J^{DSO} + J^{PSO}$. All three contributions to ^{13}C−^{1}H coupling constants were calculated with DeMon-NMR, and compared with the FC term calculated by the finite-perturbation (FPT) approach with Gaussian 98, at the respective levels mentioned above. However, since the two procedures gave very similar results only results obtained with DeMon-NMR will be presented. Full data are reported as Supporting Information.

Among the compounds studied, *o*-bromochlorobenzene is singled out as possessing a comparatively heavy atom (Br). This case was investigated in considerably more detail by computing chemical shifts (a) at the ab initio MP2/cc-pVTZ level (with Gaussian 98) and (b) exploring possible relativistic effects. To this purpose, we ran shielding calculations using the ZORA approximation[27] at the scalar and spin−orbit levels. These calculations were performed with use of the Amsterdam Density Functional (ADF) code[28] with the Becke-Perdew exchange-correlation functional[29,23b] and a triple-ζ, double polarization Slater basis set (TZ2P).[28]

The various methods used are labeled as follows: (A) P86/IGLO-III with deMon; (B) B3LYP/cc-pVTZ with Gaussian 98; (C) MP2/cc-pVTZ with Gaussian 98; (D) BP ZORA spin−orbit/TZ2P with ADF, all at the B3LYP/6-31G(d,p) geometry. The respective values of σ_{ref} (TMS) (in ppm) are the following: for ^{1}H, 31.3 (A), 31.6 (B), 31.5 (C), 31.5 (D); for ^{13}C, 179.2 (A), 183.6 (B), 198.0 (C), 185.9 (D).

2D spectra and 1D traces were simulated with Bruker NMR-SIM. 1D traces were simulated as follows: spin systems were first built from the calculated chemical shifts and *J* couplings (*weak* mode) by selecting the appropriate carbon and hydrogen nuclei. On these spin systems, single-pulse-acquire experiments were run and the output spectra were postprocessed by applying an exponential line broadening and by shifting their center to 0 Hz.

Results and Discussion

To compare calculated and experimental results, accurate J_{CH} couplings must be extracted from experimental spectra.[30] This is not a trivial problem, since only direct couplings ($^1J_{CH}$) can be detected as satellite peaks of strong ^{1}H signals, and even these are generally complicated and made less intense by the smaller long-range couplings. On the other hand, typical 2D heterocorrelated pulse sequences exploit these couplings to produce the desired coherences, but the spectra are acquired with ^{1}H or ^{13}C decoupling, thereby losing this information. Therefore, we have resorted to heteronuclear *J*-resolved sequences despite their decline in popularity, because these experiments directly furnish the *J*-coupling pattern for each signal, so that 1D traces extracted from such spectra often allow the extraction of J_{CH} values, or are suitable for visual comparison with spectra simulated with calculated values. However, they provide no chemical shift or connectivity information since the F1 dimension contains only *J*-modulated frequencies.

Furan. In Figure 1 we show the experimental (a) and simulated (b) full *J*-resolved spectra of furan. We note a very good visual similarity between the two. The corresponding data are given in Table 1.

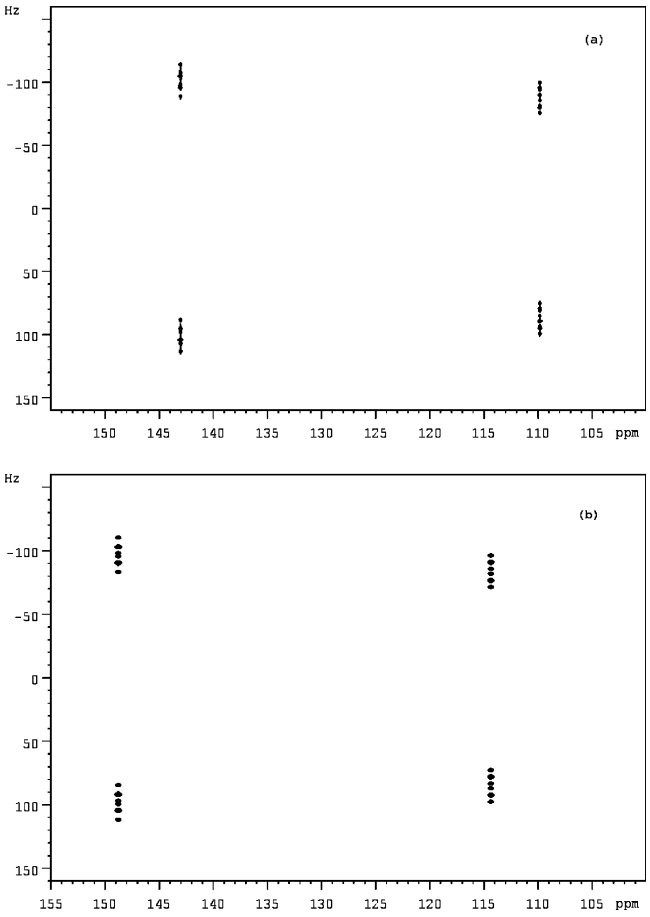

Figure 1. (a) Experimental and (b) simulated full *J*-resolved spectra of furan. The NMR parameters used for the simulation are reported in Table 1, method A.

Apart from the obvious large splitting due to direct CH couplings, extracting smaller couplings is not straightforward even in this simple system. However, since ^{13}C satellites do not cross each other, it is possible to run a selective heteronuclear *J*-resolved spectrum with inversion of one ^{1}H multiplet at a time. Selective inversion of a proton resonance results in both a simplified spectral pattern and a higher F1 resolution, provided that satellite resonances are effectively cut off by the shaped pulse. Thus, in Figure 2a we show the trace at δ 142.6 ppm extracted from the full *J*-resolved spectrum while in Figure 2b we show the same trace from the spectrum obtained with selective inversion of proton mutiplet at 6.45 ppm (H2,3); Figure 2c corresponds to selective inversion of the protons at 7.64 ppm (H1,4). Comparison of panel a in Figure 2 with panels b and c shows the advantages of using a selective rather than a hard π pulse, since narrowing the F1 spectral window leads to a higher resolution spectrum from which the desired information ($^{n}J_{CH}$) can be readily extracted. Thus, Figure 2b only contains $^{2}J_{C1,H2}$ (11.2 Hz) and $^{3}J_{C1,H3}$ (7.0 Hz), whereas Figure 2c shows only $^{3}J_{C1,H4}$ (6.9 Hz). Similar results are obtained for the trace at δ 109.4 (C2,3) (Figure 3).

TABLE 1: Calculated and Experimental Chemical Shifts and Coupling Constants of Furan[a]

	δ_{calc}(A)	δ_{calc}(B)	δ_{expt}
C1	148.8	148.2	142.6
C2	114.4	114.7	109.4

	J_{cal}(A)				J_{calc}(B)	
	TOT	FC	PSO	DSO	FC	J_{expt}
$^{1}J_{C1,H1}$	194.5	193.6	−0.1	1.0	189.2	201.7
$^{2}J_{C1,H2}$	12.3	13.5	−0.8	−0.4	13.5	11.2
$^{3}J_{C1,H3}$	7.0	7.2	0.5	−0.7	5.7	7.0
$^{3}J_{C1,H4}$	7.6	7.8	0.5	−0.7	7.0	6.9
$^{2}J_{C2,H1}$	14.2	15.1	−0.3	−0.6	11.8	14.0
$^{1}J_{C2,H2}$	168.6	167.2	0.5	0.8	162.8	174.7
$^{2}J_{C2,H3}$	4.9	5.6	−0.3	−0.4	4.6	4.2
$^{3}J_{C2,H4}$	5.6	5.8	0.4	−0.6	6.9	5.8

[a] Chemical shifts are given in ppm (ref TMS) and coupling constants in Hz.

^{13}C shifts are systematically too deshielded by about 6 ppm (<5%), so that the $\Delta\delta$(C1−C2) is essentially correct (34.4 vs 33.2 ppm). Direct $^{1}J_{CH}$ couplings are underestimated by about 7 Hz (3.5%). Hence, the agreement between experimental and calculated data is good. We can now make a first assessment of the relative contribution of the FC term (J^{FC}) and spin−orbit terms ($J^{DSO} + J^{PSO}$) to the total coupling. $^{1}J_{CH}$ and $^{3}J_{CH}$ show a similar behavior to J_{HH} couplings,[16] where the dominant contribution is J^{FC}; this is because J^{DSO} and J^{PSO} are either very small compared to J^{FC} (direct couplings) or they cancel out,

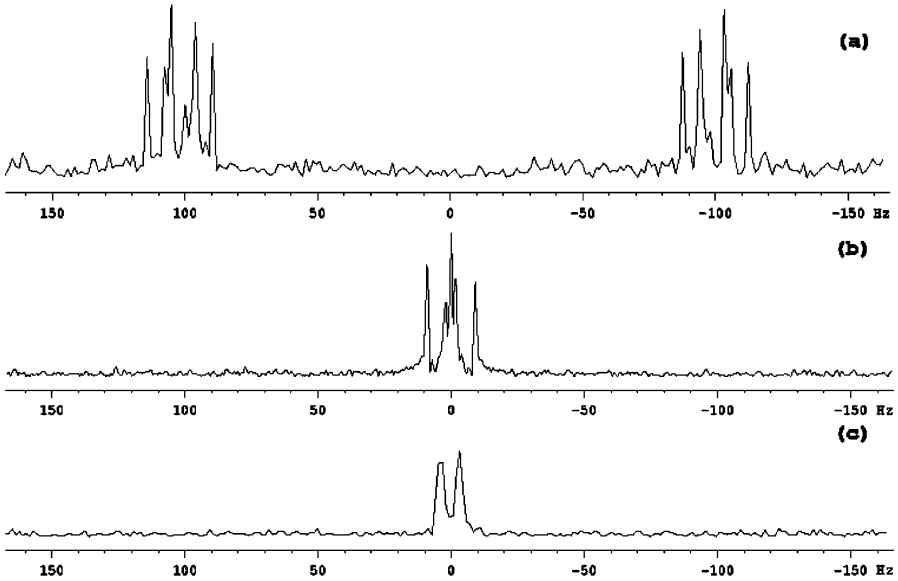

Figure 2. Trace extracted at δ 142.6 ppm (C1,4) from heteronuclear *J*-resolved spectra of furan: (a) full spectrum; (b) spectrum with selective inversion of the proton resonance at 6.45 ppm (H2,3) [the spike at 0 Hz is an experimental artifact, probably due to unmodulated residual magnetization (see also Figure 3c)]; and (c) spectrum with selective inversion of the proton resonance at 7.64 ppm (H1,4).

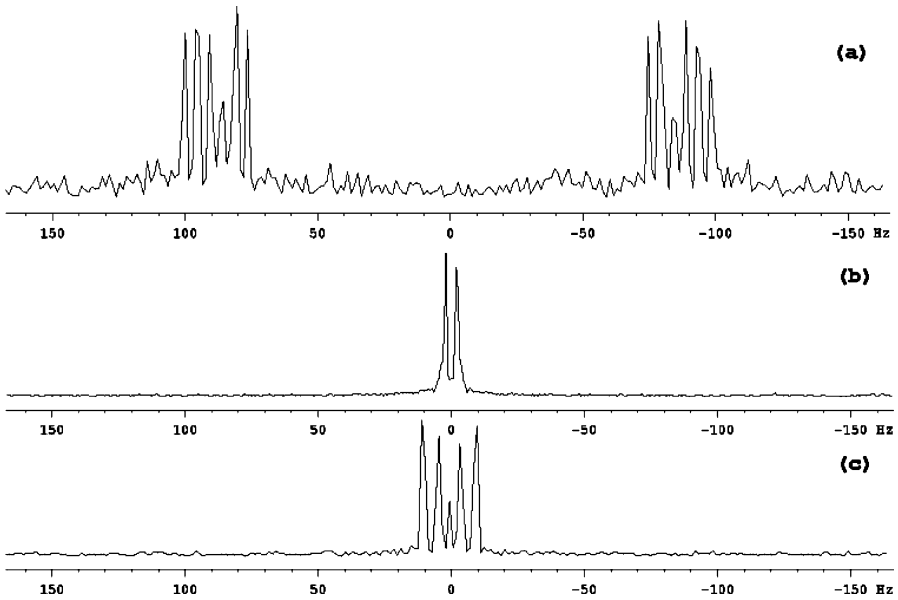

Figure 3. Trace extracted at δ 109.4 (C2,3) from heteronuclear *J*-resolved spectra of furan: (a) full spectrum; (b) spectrum with selective inversion of the proton resonance at δ 6.45 (H2,3); and (c) spectrum with selective inversion of the proton resonance at δ 7.64 (H1,4).

even though their size may not be negligible (three-bond couplings).[9,13] In contrast, for two-bond couplings J^{DSO} and J^{PSO} have the same sign and add up to a contribution of 1.0−1.5 Hz. This has a significant effect on the total coupling, since $^2J_{CH}$ is often small. The inclusion of spin−orbit contributions therefore substantially improves the agreement with experimental results for $^2J_{CH}$ (see Table 1), while the same contributions to direct and three-bonds coupling constants are much smaller.

***o*-Dichlorobenzene.** As for furan, the *J*-resolved spectrum of *o*-dichlorobenzene is complicated. Apart from the large splittings generated by direct couplings, several smaller $^nJ_{CH}$ values give rise to complex patterns that remain mostly unresolved, mainly because of low resolution in F1. Simplifying the patterns by means of selective inversion turned out to be critical, since efficient cutoff of all satellites would require very small selective pulse bandwidths, resulting in long irradiation times. Therefore, only direct couplings are explicitly obtained from our experiments; the remaining long-range coupling constants are taken from ref 31 where they have been determined by spectral simulation. Data are also presented as a comparison between F1 traces extracted along each carbon resonance and the corresponding ones simulated with calculated values, as for the case of furan. Line broadenings of simulated traces were set to values smaller than the experimental resolution in F1. The full 2D experimental (panel a) and simulated (panel b) spectra are presented in Figure 4, and numerical data are given in Table 2 (the full list of data, including FC, PSO, and DSO terms, for *o*-dichlorobenzene and all the remaining molecules are collected in the Supporting Information).

From a computational viewpoint, this molecule is a stringent test since the three ^{13}C signals lie within only 3.5 ppm of each other. All calculated shifts are again too deshielded, but chlorine-bonded carbons show a larger deviation (13%) than the others, for which the deviation is similar to the previous results. A similar trend was also found in the other halogenated molecules examined (see below). As a result the ordering of signals is correct, but the calculated $\Delta\delta$(C1−C4) (17 ppm) is much larger than found. Calculated $^1J_{CH}$ values are underestimated by 8−9 Hz, i.e lie within ca. 5% of the experimental value. Once again, $^2J_{CH}$ coupling constants have a contribution of 1.0−1.5 Hz from spin−orbit terms, while the other couplings are essentially determined only by the FC contribution. Calculated and experimental ^{13}C NMR parameters are collected in Table 2. As mentioned above, it was not possible to extract long-range couplings from the spectra. Therefore, the calculations are evaluated comparing 1D traces (Figure 5).

TABLE 2: Calculated and Experimental Chemical Shifts and Coupling Constants of *o*-dichlorobenzene[a,b]

	δ_{calc}(A)	δ_{calc}(B)	δ_{expt}
C1	150.2	148.7	132.3
C3	137.4	136.9	131.0
C4	133.2	132.4	128.8
	J_{calc}(A)	J_{calc}(B)	J_{expt}
$^3J_{C1,H3}$	7.8	7.8	7.9
$^4J_{C1,H4}$	−1.2	−1.3	
$^3J_{C1,H5}$	11.2	11.1	11.6
$^2J_{C1,H6}$	−2.2	−1.0	−3.5
$^1J_{C3,H3}$	158.8	155.5	167.0
$^2J_{C3,H4}$	3.6	4.1	1.9
$^3J_{C3,H5}$	8.2	8.1	8.4
$^4J_{C3,H6}$	−0.8	−0.7	
$^2J_{C4,H3}$	1.6	2.3	0.0
$^1J_{C4,H4}$	155.1	152.4	164.5
$^2J_{C4,H5}$	2.6	3.2	1.1
$^3J_{C4,H6}$	8.5	8.2	8.6

[a] Chemical shifts are given in ppm (ref TMS) and coupling constants in Hz. [b] Experimental $^nJ_{CH}$ from ref 31.

Figure 5a displays the coupling pattern of C4,5. In the simulated trace, the larger splitting is due to the $^1J_{CH}$ coupling, while the smaller splittings are generated by the $^3J_{CH}$ and broadened by additional unresolved long-range $^2J_{CH}$ couplings. Figure 5b represents the heteronuclear coupling pattern of C3,6. In this case, since the difference between coupling constants is larger than the spectral resolution, a clearer splitting pattern is observed. The simulated trace is produced by the large $^1J_{CH}$ coupling, further split by $^3J_{CH}$, and again by $^2J_{CH}$. In both cases, the simulated patterns closely match the experimental ones. Finally, in Figure 5c we show the trace of the quaternary carbons C1,2. The simulated trace correctly shows the side doublets, while the central region is split into four peaks rather than two. This disagreement probably reflects the discrepancy between experimental and calculated values of the smallest coupling constants ($^2J_{C1,H6}$ and, possibly, $^4J_{C1,H4}$ for which there is no experimental value; see Table 2).

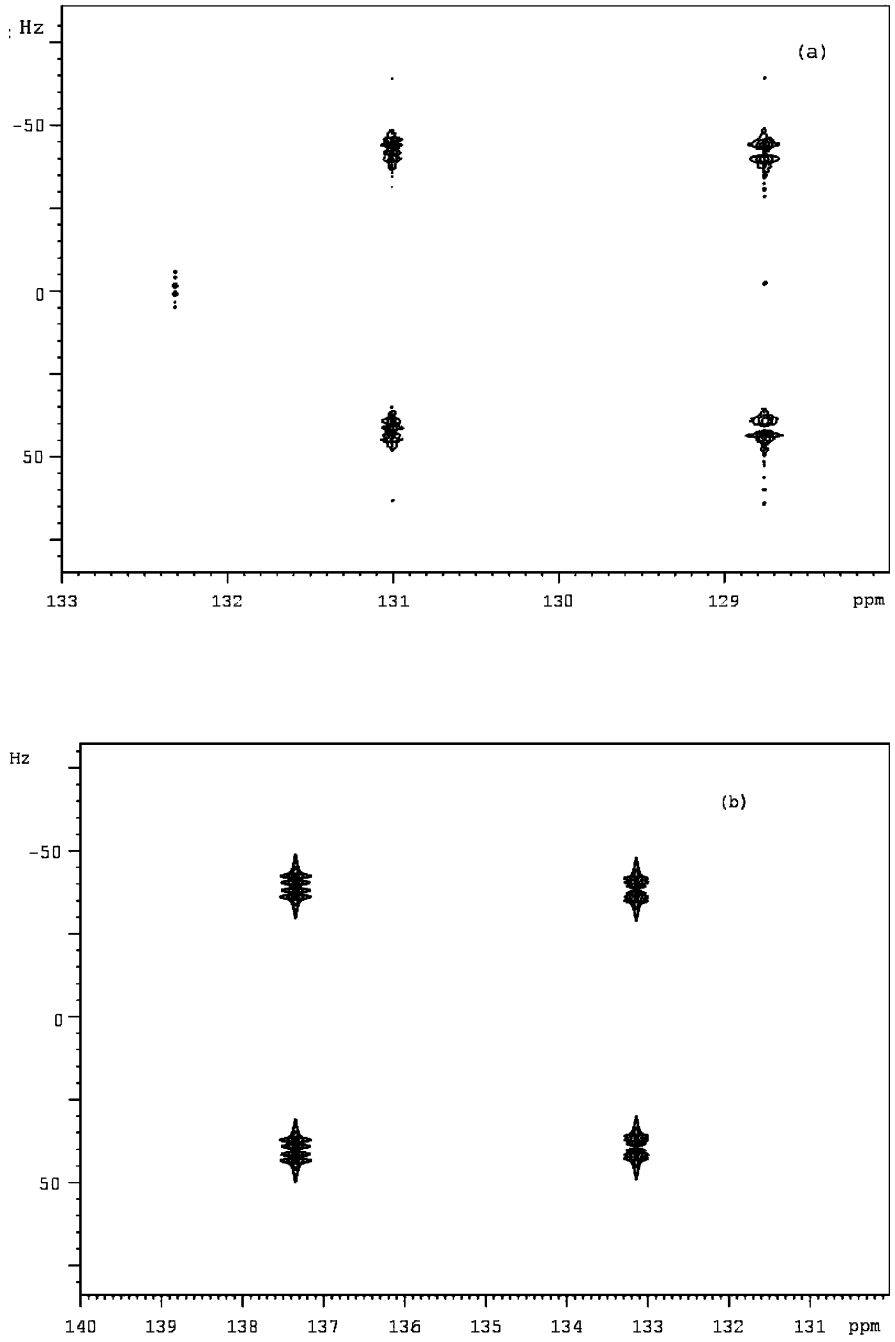

Figure 4. (a) Experimental full *J*-resolved spectrum of *o*-dichlorobenzene. Since a gated-decoupled pulse sequence was used, the F1 dimension displays *J*/2 instead of *J*. (b) Simulated *J*-resolved spectra of *o*-dichlorobenzene excluding the signal of quaternary carbons which are calculated too deshielded. The NMR parameters used for the simulation are reported in Table 2, method A.

The comparison of calculated long-range coupling constants with those reported in ref 31 shows a very good agreement concerning three-bond couplings, while a worse correlation is found with two-bond coupling constants.

***o*-Bromochlorobenzene**. The spectrum of this molecule features six ^{13}C signals spanning only 12.1 ppm, in the order C6 $\approx$ C2 > C3 > C4 > C5 > C1. In the calculated series C1 falls between C2 and C6, while the remaining signals follow the experimental ordering (Table 3).

Thus, the calculated chemical shift of C1 (bound to Br) is again too deshielded compared to experiment, but to a larger extent (149.3 vs 122.2 ppm), while for carbons bound to Cl and H the deviations are similar to those previously observed. Since this is the only system containing a fairly heavy atom, we further investigated it in two ways. First we tried to improve the treatment of electron correlation through a calculation of the chemical shift at the ab initio MP2/cc-pVTZ level (method C). A substantial improvement (138.8 and 144.0 ppm, for C1 and C2, respectively) was obtained, indicating that electron correlation certainly needs a more accurate treatment than in the other molecules. At the MP2 level of theory the average absolute error for ^{13}C chemical shifts is reduced to just 5.1 ppm, in contrast to an average error of 11.2 ppm at the DFT level. However, the order of the ^{13}C resonances is still not completely correct.

We then proceeded to check for the influence of relativistic effects by computing shieldings (also of the reference TMS) at the relativistic spin−orbit ZORA level (method D).[32] This calculation yielded the spin−orbit contribution to the nuclear shielding (i.e., now $\sigma = \sigma_d + \sigma_p + \sigma_{SO}$), with σ_{SO}(C1) = 11.6

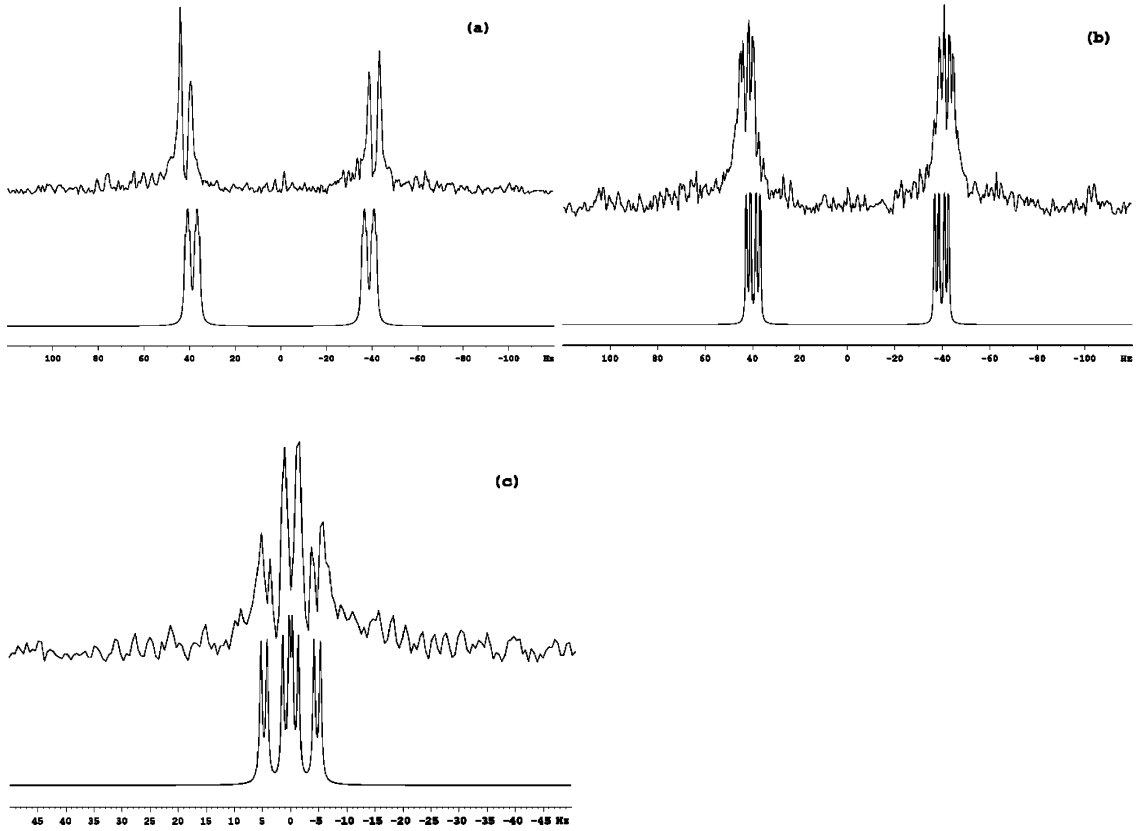

Figure 5. Traces extracted from the *J*-resolved spectrum of *o*-dichlorobenzene: (top) experimental [since a gated-decoupled pulse sequence was used, the F1 dimension displays *J*/2 instead of *J*]; (bottom) calculated at δ (a) 128.8 (C4,5), (b) 131.0 (C3,6), and (c) 132.3 (C1,2).

ppm. As expected, for the chlorine-bonded carbon (C2) σ_{SO} is much smaller (2.9 ppm), even smaller for the other carbons (<0.5 ppm; see Supporting Information), and σ_{SO}(TMS) = 0.9 ppm. After this correction, δ(C1) = 139.7 ppm, in much better agreement with experiment (Table 3). We remark that the calculation at the relativistic scalar (spin-free) ZORA level did not improve the result, which shows that the disagreement noted at the nonrelativistic levels is due to the neglect of spin−orbit coupling. The ordering of signals after this correction is C2 > C6 > C1 > C3 > C4 > C5, i.e., the shift of C1 is still not satisfactory.

"Heavy-atom effects" on the chemical shift of a light nucleus bonded to a heavy one are well documented in the literature, both experimentally and theoretically,[18] but most often for cases where several heavier atoms are present (e.g. CI_4, PI_4^+; in such cases, σ_{SO} amounts to hundreds of ppm). On the contrary, the above data indicate that relativistic effects may be relevant even in molecules containing just one Br atom, which calls for caution whenever such molecules are considered, and great accuracy is desired. The rather large effect can probably be related to the high s character of the C−Br sp^2 bond, consistent with the increasing σ_{SO} values in the series iodoethane, iodoethylene, and iodoacetylene (respectively 26.2, 33.6, and 56.7 ppm) calculated by Kaupp et al.[18a]

Remarkably, by adding the σ_{SO} term to the MP2 results of column C the order C2 > C6 > C3 > C4 > C5 > C1 is found, which is the best agreement with experiment we could obtain. Obviously, the assumption of additivity of MP2 shieldings ($\sigma_d + \sigma_p$) to a spin−orbit term obtained by DFT has no firm theoretical ground. However, this result indicates that (a) MP2 is superior to DFT in computing the treatment of electron correlation in molecules containing Cl or Br (indeed, a better performance of MP2 vs DFT for ^{13}C chemical shifts has already been observed for a set of molecules containing only light atoms[33]) and (b) the SO contribution to the total shielding is not negligible and may have to be added to the typical dia- and paramagnetic terms. However, the MP2 calculation is so demanding on disk and memory resources that even slightly larger molecules than those dealt with here are, at present, hardly tractable.

We further show the beneficial effect of calculating NMR parameters by analyzing the line width of the C1 and C2 signals. Both are substantially broader (shorter T_2) than those of C3−6, owing to scalar coupling to the quadrupolar nuclei ^{79,81}Br and ^{35,37}Cl (all with $I = {}^3/_2$), respectively, but the former signal is narrower. The shorter T_2 arises from a combination of the fast relaxation of the quadrupolar nuclide (T_{2X}, X = ^{79,81}Br or ^{35,37}Cl) and the magnitude of the J_{CX} coupling constant through the expression for relaxation by scalar coupling[34]

$$\frac{1}{T_{2C}} = \frac{4\pi^2}{3} J_{CX}{}^2 I_X (I_X + 1)\left[T_{2X} + \frac{T_{2X}}{1 + (\Delta\omega)^2 T_{2X}{}^2}\right]$$

where I_X refers to the quadrupolar nuclide, and $\Delta\omega$ is the difference of Larmor frequencies, $\Delta\omega = \omega(^{13}C) - \omega(X)$. The term depending on $\Delta\omega$ (scalar relaxation of the second kind) is generally negligible, with the notable exception of ^{13}C−^{79}Br coupling.[34] T_{2X} cannot be determined directly, because the halogen signals are too broad. However, it can be estimated through standard formulas, which yield T_{2X} values of 46, 74, 0.68, and 1.08 μs for ^{35}Cl, ^{37}Cl, ^{79}Br, and ^{81}Br, respectively, mainly as a consequence of the smaller quadrupole moment of chlorine isotopes.[35] The calculated (relativistic ZORA Spin−Orbit/TZ2P level) coupling constants with ^{13}C are −34, −28, −140, and −151 Hz, respectively. Inserting these values in the above equation, one gets a line widths ratio $W_{1/2}$(C1)/$W_{1/2}$(C2) of 0.4, in perfect agreement with the experimental line width

TABLE 3: Calculated and Experimental Chemical Shifts and Coupling Constants of *o*-bromochlorobenzene[a,b]

	δ_{calc}(A)	δ_{calc}(B)	δ_{calc}(C)	δ_{calc}(D) (σ_{SO})	δ_{expt}
C1	149.3	147.6	138.8	139.7 (11.6)	122.2
C2	152.5	151.2	144.0	149.3 (2.9)	134.2
C3	137.5	136.8	133.2	136.2 (1.0)	130.9
C4	133.8	133.2	129.5	132.2 (0.5)	129.4
C5	132.9	132.3	129.0	131.6 (0.4)	128.9
C6	141.0	140.2	136.0	140.2 (0.0)	134.3

	J_{calc}(A)	J_{calc}(B)
$^3J_{C1-H3}$	7.8	7.7
$^4J_{C1-H4}$	−1.2	−1.3
$^3J_{C1-H5}$	11.5	11.2
$^2J_{C1-H6}$	−1.9	−0.7

	δ_{calc}(A)	δ_{calc}(B)	δ_{expt}
$^2J_{C2-H3}$	−2.1	−0.9	
$^3J_{C2-H4}$	11.2	11.1	12.3
$^4J_{C2-H5}$	−1.2	−1.3	
$^3J_{C2-H6}$	8.4	8.2	
$^1J_{C3-H3}$	159.2	155.6	166.5
$^2J_{C3-H4}$	3.6	4.1	4.1
$^3J_{C3-H5}$	8.2	8.0	8.2
$^4J_{C3-H6}$	−0.9	−0.7	
$^2J_{C4-H3}$	1.6	2.3	
$^1J_{C4-H4}$	155.2	152.2	165.5
$^2J_{C4-H5}$	2.7	3.2	
$^3J_{C4-H6}$	8.6	8.2	9.0
$^3J_{C5-H3}$	8.4	8.1	8.2
$^2J_{C5-H4}$	2.7	3.2	
$^1J_{C5-H5}$	155.8	152.4	165.5
$^2J_{C5-H6}$	1.5	2.4	
$^4J_{C6-H3}$	−0.7	−0.6	
$^4J_{C6-H4}$	8.2	8.0	9.3
$^2J_{C6-H5}$	3.7	4.1	2.1
$^1J_{C6-H6}$	159.9	156.0	167.5

[a] Chemical shifts are given in ppm (ref TMS) and coupling constants in Hz. [b] Some experimental data are missing, also in the following tables, either because the trace of the quaternary carbon is not visible in the *J*-resolved spectrum, or because the values are below the experimental resolution.

ratio (which is also 0.4) obtained from Lorentian fitting of the experimental ^{13}C spectrum.

Dichlorophenols (DCP). In all isomers investigated, the six nonequivalent ^{13}C signals span a moderate range ($\Delta\delta$ < 40 ppm) and always appear with C1 and C6 having the largest and the smallest chemical shift, respectively. Similarly to the previous cases, *J*-resolved spectra provided complex multiplets, and it was only rarely possible to run selective experiments to assign long-range couplings ($^3J_{C4,H2}$ and $^3J_{C3,H5}$ in 3,4-DCP); experimental coupling constants have been assigned mostly by comparison with the calculated values. For brevity, the results are only tabulated in the Supporting Information (Tables S4−S7).

Calculated chemical shifts exhibit a similar trend to the previous molecules, chlorine-bound carbons having again the largest deviation. Coupling constants conform in all respects to the behavior already observed.

For all DCP's, the calculated sequence of signals always gives the correct order of the extreme signals C1 and C6. For 2,3- and 2,5-DCP, the calculated sequence of the other signals agrees with experiment, except for C2 and C4 (differing by 1.9 and 1.3 ppm, respectively), which appear in reverse order. For 3,4-DCP two signals are again interchanged (C4 and C5, $\Delta\delta$ = 9.0 ppm). 2,4-DCP, with C2−C5 lying within only 8 ppm of each other, gives the worst agreement (C4 > C5 > C2,3 instead of C3 > C5 > C4 > C2). As for the case of *o*-bromochlorobenzene, the MP2 results for 2,4-DCP are better correlated with experimental values: the average absolute error is 4.8 ppm, to be compared with an average error of 9.4 ppm at the DFT level. Some additional improvement can be obtained by taking into account spin−orbit coupling effects: for C2 and C4 σ_{SO} amount to 2.5 and 3.2 ppm, respectively. In fact, with method D the order of carbon chemical shifts is C4 > C3 > C5 > C2. Thus, even this level of theory is not sufficient to correctly calculate the ordering of all ^{13}C nuclei.

TABLE 4: Calculated and Experimental Chemical Shifts and Coupling Constants of Naphthalene[a,b]

	δ_{calc}(A)	δ_{calc}(B)	δ_{expt}
C1	135.8	133.9	128.3
C2	132.7	131.2	126.3
C10	143.0	140.8	134.1

	J_{calc}(A)	J_{calc}(B)	J_{expt}
$^1J_{C1,H1}$	151.0	148.9	158.3
$^2J_{C1,H2}$	2.4	3.2	
$^3J_{C1,H3}$	6.9	6.9	
$^4J_{C1,H4}$	−1.0	−0.9	
$^4J_{C1,H5}$	1.0	0.8	
$^3J_{C1,H8}$	5.2	5.6	
$^2J_{C2,H1}$	2.2	3.1	
$^1J_{C2,H2}$	151.8	149.2	159.3
$^2J_{C2,H3}$	2.9	3.2	
$^3J_{C2,H4}$	7.9	7.9	

[a] Chemical shifts are given in ppm (ref TMS) and coupling constants in Hz. [b] Only coupling constants used in simulations are shown. The trace relative to C10,11 is omitted since it does not appear to be *J*-modulated, mainly because of its extremely low intensity.

Naphthalene. The three nonequivalent signals appear in the order C10 > C1 > C2 (total $\Delta\delta$ = 7.8 ppm), matched by the computations. This highly symmetric molecule features several magnetically nonequivalent nuclei with very similar coupling constants, which give rise to complex patterns in the *J*-resolved spectrum (Table 4, Figure 6).

In Figure 6 we show the trace of the *J*-resolved spectrum corresponding to C2 and C1. Apart form the large splitting due to $^1J_{CH}$, it is difficult to assign (or even distinguish) all the peaks in the multiplet structure, and therefore to extract experimental long-range couplings. Although one visually notices some similarity, even minute variations in the couplings lead to large changes in the appearance of these spectra, owing to the extremely complex patterns which often are incompatible with line broadening used in data processing. The relative contributions to coupling constants again match those found for the other aromatic compounds.

Cyclohexane. The experimental and calculated results are reported in Table 5. Experimental data were obtained from low-temperature spectra of cyclohexane-d_{11}.[37] The calculated direct coupling constants ($^1J_{CHa,e}$) are underestimated by less than 5%, as generally observed for aromatic compounds. The long-range couplings $^3J_{CH}$ are also well reproduced, while larger errors are found for $^2J_{CH}$. In contrast to the previous cases, however, the DSO and PSO terms exactly cancel out also in $^2J_{CH}$.

***n*-Butyl Chloride.** Calculated chemical shifts are, as usual, too deshielded by about 5−10 ppm, i.e., an accuracy similar to that observed for aromatic compounds. Due to the smaller value of δ, this results in a larger relative error; in any event, the correct ordering is predicted.

In contrast to the previous cases, from the full *J*-resolved spectra we were able to obtain only the direct couplings, because the F1 resolution is extremely small (coupling patterns are triplets or quartets, which exhibit a smaller S/N ratio and render

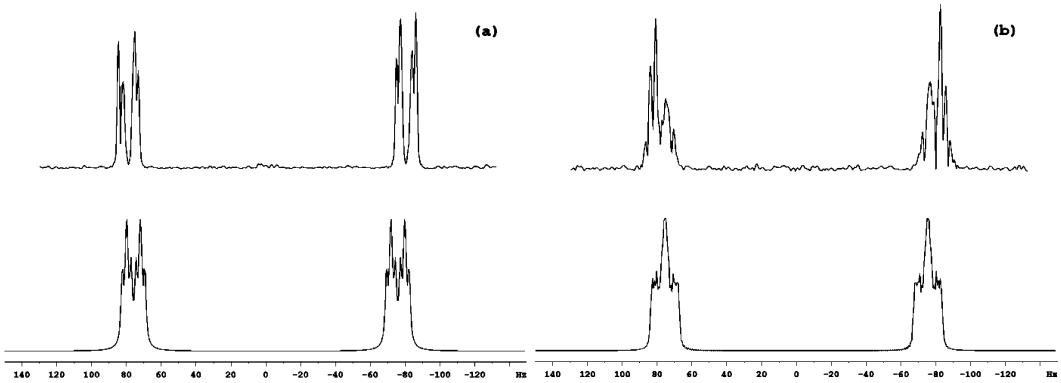

Figure 6. Traces extracted from the *J*-resolved spectrum of naphthalene: (top) experimental; (bottom) calculated at δ (a) 126.3 (C2) and (b) 128.3 (C1). In the simulated spectra, coupling constants smaller than 1 Hz were not considered, as their values are smaller than the line broadening applied along F1.

TABLE 5: Calculated and Experimental Chemical Shifts and Coupling Constants of Cyclohexane[a,b]

	δ_{calc}(A)			δ_{calc}(B)		δ_{expt}
C	34.6			31.9		27.0
	J_{calc}(A)					
	TOT	FC	PSO	DSO	J_{calc}(B)	J_{expt}
$^1J_{CHa}$	116.6	114.8	0.9	0.9	109.4	122.4
$^1J_{CHe}$	121.4	119.6	0.9	0.9	117.3	126.4
$^2J_{CHa}$	−2.2	−2.2	0.1	−0.1	−2.6	−3.9
$^2J_{CHe}$	−2.2	−2.2	0.1	−0.1	−2.6	−3.7
$^3J_{CHa}$	2.2	2.2	0.0	0.0	1.8	2.1
$^3J_{CHe}$	8.1	8.1	0.4	−0.4	7.1	8.1
$^4J_{CHa}$	−0.2	−0.2	0.1	−0.1	−0.1	−0.3
$^4J_{CHe}$	−0.5	−0.5	0.3	−0.3	−0.5	−0.5

[a] Chemical shifts are given in ppm (ref TMS) and coupling constants in Hz. [b] Experimental values from ref 37.

the F1 window much larger). It was only possible to run selective experiments on H1 and H4, which are well separated from the methylene signals, so that we could measure the long-range constants with those protons (Table 6).

The NMR parameters were first calculated considering only the all-trans conformation **10** shown in Chart 1 (conformer A). The coupling of carbons with the fast rotating methyl protons on C4 has been calculated as an average of the three values obtained from the calculation. For example, the $^3J_{C2H4}$ coupling with the trans proton is calculated to be 11.75 Hz; in contrast, $^3J_{C2H4}$ with the gauche protons is calculated to be 2.47 Hz, and the average (5.6 Hz) is in excellent agreement with experiment (5.5 Hz). To calculate the $^3J_{C3H1}$ we need to consider, in addition to conformation **10**, also the conformer where the chlorine atom is in the gauche position (conformer B; the two structures differ by only 4.6 kJ/mol at the B3LYP/6-31G(d,p) level). Again, $^3J_{C3H1}$ are different, depending on the proton position. For the gauche proton in conformer A we calculated 1.5 Hz, while for the gauche and trans protons in conformer B we obtain 3.5 and 8.4 Hz, respectively. The experimental value of 4.5 Hz is in excellent agreement with the average result obtained from the calculation. A similar large effect has been calculated for $^2J_{C2H1}$: here the coupling constant of C2 with the gauche proton in conformer A is calculated to be −5.41 Hz, while the couplings with the trans and gauche proton of conformer B are 5.09 and −4.92 Hz. Therefore the average value is strongly affected by the conformation. Finally, we note that, as found for cyclohexane, spin−orbit contributions to all coupling constants are negligible: either they are much smaller (ca. 1 Hz) than the FC term, as for the $^1J_{CH}$, or they almost exactly cancel out for the long-range coupling constants.

TABLE 6: Calculated and Experimental ^{13}C Chemical Shifts and J_{CH} Coupling Constants of *n*-Butyl Chloride[a,b]

	δ_{calc}(A)	Δ_{calc}(B)	δ_{expt}
C1	57.7	55.1	45.2
C2	44.5	42.1	35.0
C3	28.2	27.1	20.4
C4	17.0	16.5	13.7
	J_{calc}(A)	J_{calc}(B)	J_{expt}
$^1J_{C1-H1}$	140.2	135.9	150.2
$^2J_{C1-H2}$	−1.7	−5.4	
$^3J_{C1-H3}$	2.5	2.1	
$^4J_{C1-H4}$	0.5	1.1	
$^2J_{C2-H1}$	−0.7	−1.9	3.0
$^1J_{C2-H2}$	120.7	118.2	130.6
$^2J_{C2-H3}$	−2.5	−3.0	
$^3J_{C2-H4}$	5.6	5.0	5.5
$^3J_{C3-H1}$	4.5	1.3	4.5
$^2J_{C3-H2}$	−2.5	−3.2	
$^1J_{C3-H3}$	119.2	113.7	125.7
$^2J_{C3-H4}$	−2.4	−3.1	4.4
$^4J_{C4-H1}$	−0.1	−0.2	
$^3J_{C4-H2}$	2.3	2.2	
$^2J_{C4-H3}$	−2.4	−3.1	
$^1J_{C4-H4}$	119.5	115.2	124.5

[a] Chemical shifts are given in ppm (ref TMS) and coupling constants in Hz. [b] All values with method A are calculated as averages between conformer A (**10**) and conformer B (with chlorine in the gauche position). Values with method B are for conformer A only. All magnetically equivalent protons are also averaged in the calculation of $^nJ_{CH}$.

General Assessment of the Calculated Values. We have shown that the calculations provide results suitable for structure elucidation, for example through direct simulation with typical 2D pulse sequences. Some issues remain open, however: the accuracy of computed chemical shifts of carbon nuclei bonded to Cl and Br (a common situation in organic chemistry) is much lower than that of proton- and carbon-bonded ones, so that the assignment of closely spaced groups of such peaks may be questionable if the chemical shift range is smaller than ca. 10 ppm. In contrast, molecules not containing halogens are much better modeled (e.g. naphthalene, where the ordering is correct despite a $\Delta\delta$ of 8 ppm). The case of *o*-bromochlorobenzene is particularly informative, since it has highlighted that relativistic effects, commonly thought to be relevant only for the heavier halogen iodine, are not negligible and should be taken into account. On the other hand, the quality of computed coupling constants is always good, so that, in general, the latter calculation poses fewer problems than that of δ.

Another important unsolved issue concerns solvent effects, since all NMR spectra (and especially chemical shifts) are, to

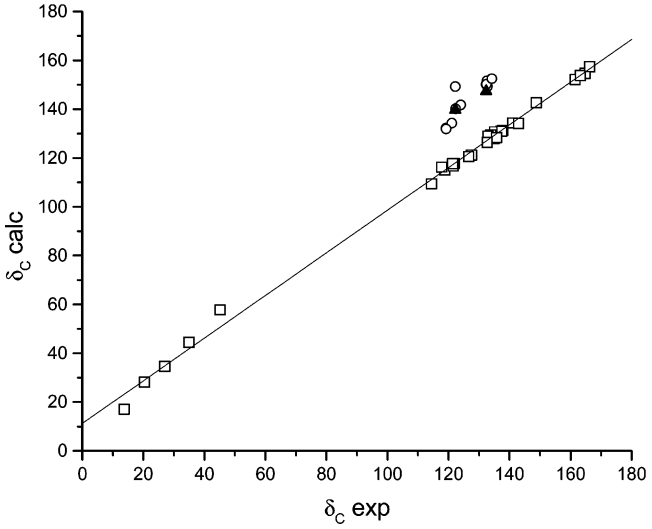

Figure 7. Correlation between experimental and calculated (method A) ^{13}C chemical shifts: (open squares) carbon atoms bonded to carbon or hydrogen with linear fitting $\delta_{calc} = a\delta_{exptl} + b$ ($a = 0.87 \pm 0.01$, $b = -11 \pm 1$, $r = 0.998$); (open circles) carbon atoms bonded to chlorine or bromine; (filled triangles) C1(Br) and C2(Cl) atoms of *o*-bromochlorobenzene (relativistic method D). The average absolute deviation is 6.0 ppm for carbons bonded to light atoms, and 16.4 ppm for chlorinated carbons.

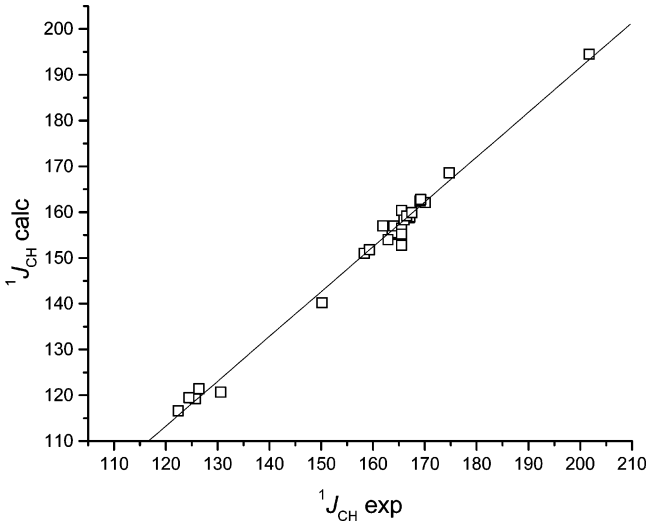

Figure 8. Correlation between experimental and calculated (method A) direct $^1J_{CH}$ coupling constants, with linear fitting $J_{calc} = aJ_{exptl} + b$ ($a = 0.98 \pm 0.02$, $b = -4 \pm 3$, $r = 0.996$). The average absolute deviation is 7.6 Hz.

some extent, affected by the solvent, viz. the well-known, if outdated, usage of benzene solvent as a workaround to disentangle crowded spectral regions. In this study solvent effects have been neglected in the calculations. The main reason is that the molecules investigated are nonpolar or weakly polar, and as such, can be expected to undergo relatively small solvent effects, provided that the solvent is itself slightly polar, noncoordinating, and has a negligible magnetic anisotropy. However, this issue should be kept in mind whenever these conditions do not apply, e.g. when dealing with strongly polar molecules, whose spectra have to be run in polar solvents. In such cases, one should expect major effects on all spectral parameters, arising both directly or indirectly through changes in the molecular structure, to an extent that may seriously limit the applicability of the computational protocol we have presented.

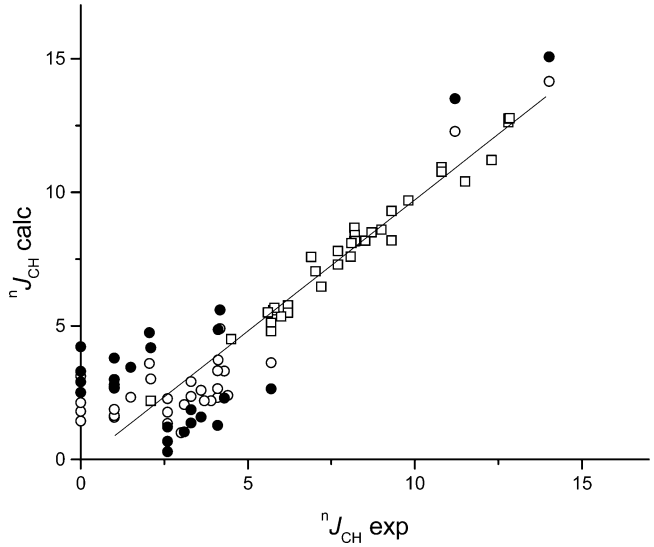

Figure 9. Correlation between experimental and calculated (method A) geminal and vicinal $^nJ_{CH}$ ($n = 2, 3$) coupling constants: (open squares) $^3J_{CH}$ with linear fit $J_{calc} = aJ_{exptl} + b$ ($a = 0.98 \pm 0.02$, $b = -0.1 \pm 0.2$, $r = 0.985$); (open circles) $^2J_{CH}$, total value (no fitting); (solid circles) $^2J_{CH}$, FC contribution only. The average absolute deviation is 0.4 Hz for $^3J_{CH}$ and 1.2 Hz for $^2J_{CH}$, while the error is doubled (2.1 Hz) if we consider only the FC contribution to $^2J_{CH}$.

To summarize our results, in Figures 7−9 we report the general correlation between experimental and theoretical results. Aromatic and aliphatic ^{13}C chemical shifts (Figure 7) are clearly distinguished. Relativistic effects are also visible for C1 and C2 of *o*-bromochlorobenzene. Direct coupling constants are also well correlated (Figure 8). Finally, in Figure 9 the better correlation for three-bond coupling constants compared to two-bond coupling constants is apparent. However, it is also clear that inclusion of the DSO and PSO contributions in $^2J_{CH}$ substantially improves the agreement, so that the calculation of these additional terms is certainly justified.

Conclusions

We have obtained accurate experimental values of $\delta(^{13}C)$ and $^nJ_{CH}$ in a sample of common organic functional groups, and compared them with the corresponding values calculated by several DFT methods, up to relativistic spin−orbit contributions in appropriate cases. Whereas many similar studies have recently been, and are being, undertaken, most such endeavors have usually focused on the calculation of either δ or J, often for a single molecule or a small homogeneous group thereof. On the contrary, we strived to provide a comprehensive computational protocol aimed at predicting both δ and J values in a rather broad range of chemical environments, while at the same time analyzing the involved factors. Despite some shortcomings concerning halogen-bonded carbon nuclei, the proposed protocol performs remarkably well, providing reliable results quite efficiently, thus enabling the NMR spectra of larger molecules to be directly synthesized.

Acknowledgment. We thank V. G. Malkin and O. L. Malkina for providing us with the software code deMon-NMR and Dr. S. Boschi at the CINECA Supercomputer Center for his help with MP2 calculations on the IBM SP4.

Supporting Information Available: Calculated shieldings and components of spin−spin couplings for all compounds. This

material is available free of charge via the Internet at http://pubs.acs.org.

References and Notes

(1) Kalinowski, H.; Berger, S.; Braun, S. *^{13}C NMR Spektroskopie*; Georg Thieme Verlag: Stuttgart, Germany, 1984.

(2) Helgaker, T.; Jaszuński, M.; Ruud, K. *Chem. Rev.* **1999**, *99*, 293.

(3) Backes, A. C.; Schatz, J.; Siehl, H.-U. *J. Chem. Soc., Perkin Trans. 2* **2002**, 484.

(4) (a) Kaupp, M.; Malkin, V. G.; Malkina, O. L.; Salahub, D. R. *Chem. Eur. J.* **1996**, *2*, 24. (b) Wiberg, K. B.; Hammer, J. D.; Zilm, K. W.; Cheeseman, J. R. *J. Org. Chem.* **1999**, *64*, 6394.

(5) (a) Barone, G.; Gomez-Paloma, L.; Duca, D.; Silvestri, A.; Riccio, R.; Bifulco, G. *Chem. Eur. J.* **2002**, *8*, 3233. (b) Barone, G.; Duca, D.; Silvestri, A.; Gomez-Paloma, L.; Riccio, R.; Bifulco, G. *Chem. Eur. J.* **2002**, *8*, 3240.

(6) Vrček, V.; Kronja, O.; Siehl, H.-U. *J. Chem. Soc., Perkin Trans. 2* **1999**, 1317.

(7) (a) Bagno, A. *Chem. Eur. J.* **2000**, *6*, 2925. (b) Barfield, M. *J. Am. Chem. Soc.* **2002**, *124*, 4158. (c) Pecul, M.; Sadlej, J.; Helgaker, T. *Chem. Phys. Lett.* **2003**, *372*, 476.

(8) (a) Bagno, A.; Saielli, G.; Scorrano, G. *Angew. Chem., Int. Ed.* **2001**, *40*, 2532. (b) Bagno, A.; Saielli, G.; Scorrano, G. *Chem. Eur. J.* **2002**, *8*, 2047.

(9) (a) Church, T. J.; Carmichael, I.; Serianni, A. S. *J. Am. Chem. Soc.* **1997**, *119*, 8946. (b) Cloran, F.; Carmichael, I.; Serianni, A. S. *J. Phys. Chem.* **1999**, *103*, 3783. (c) Cloran, F.; Zhu, Y.; Osborn, J.; Carmichael, I.; Serianni, A. S. *J. Am. Chem. Soc.* **2000**, *122*, 6435. (d) Stenutz, R.; Carmichael, I.; Widmalm, G.; Serianni, A. S. *J. Org. Chem.* **2002**, *67*, 949.

(10) Malkin, V. G.; Malkina, O. L.; Salahub, D. R. *Chem. Phys. Lett.* **1994**, *221*, 91.

(11) Jaszuński, M.; Ruud, K. *Chem. Phys. Lett.* **2001**, *336*, 473.

(12) Krivdin, L. B.; Sauer, S. P. A.; Peralta, J. E.; Contreras, R. H. *Magn. Reson. Chem.* **2002**, *40*, 187.

(13) Czernek, J.; Lang, J.; Sklenár, V. *J. Phys. Chem. A* **2000**, *104*, 2788.

(14) Malkina, O. L.; Hricovíni, M.; Bizik, F.; Malkin, V. G. *J. Phys. Chem. A* **2001**, *105*, 9188.

(15) Wu, A.; Cremer, D.; Auer, A. A.; Gauss, J. *J. Phys. Chem. A* **2002**, *106*, 657.

(16) Bagno, A. *Chem. Eur. J.* **2001**, *7*, 1652.

(17) Tähtinen, P.; Bagno, A.; Klika, K. D.; Pihlaja, K. *J. Am. Chem. Soc.* **2003**, *125*, 4609.

(18) (a) Kaupp, M.; Malkina, O. L.; Malkin, V. G.; Pyykkö, P. *Chem. Eur. J.* **1998**, *4*, 118. (b) Kaupp, M.; Malkina, O. L.; Malkin, V. G. *Chem. Phys. Lett.* **1997**, *265*, 55. (c) Malkin, V. G.; Malkina, O. L.; Salahub, D. R. *Chem. Phys. Lett.* **1996**, *261*, 335.

(19) Claridge,T. D. W. *High-Resolution NMR Techniques in Organic Chemistry*; Pergamon: Oxford, UK, 1999; p 260.

(20) Bax, A.; Freeman, R. *J. Am. Chem. Soc.* **1982**, *104*, 1099.

(21) (a) Becke, A. D. *J. Chem. Phys.* **1996**, *104*, 1040. (b) Lee, C.; Yang, W.; Parr, R. G. *Phys. Rev. B* **1988**, *37*, 785.

(22) Frisch, M. J.; Trucks, G. W.; Schlegel, H. B.; Scuseria, G. E.; Robb, M. A.; Cheeseman, J. R.; Zakrzewski, V. G.; Montgomery, J. A., Jr.; Stratmann, R. E.; Burant, J. C.; Dapprich, S.; Millam, J. M.; Daniels, A. D.; Kudin, K. N.; Strain, M. C.; Farkas, O.; Tomasi, J.; Barone, V.; Cossi, M.; Cammi, R.; Mennucci, B.; Pomelli, C.; Adamo, C.; Clifford, S.; Ochterski, J.; Petersson, G. A.; Ayala, P. Y.; Cui, Q.; Morokuma, K.; Malick, D. K.; Rabuck, A. D.; Raghavachari, K.; Foresman, J. B.; Cioslowski, J.; Ortiz, J. V.; Stefanov, B. B.; Liu, G.; Liashenko, A.; Piskorz, P.; Komaromi, I.; Gomperts, R.; Martin, R. L.; Fox, D. J.; Keith, T.; Al-Laham, M. A.; Peng, C. Y.; Nanayakkara, A.; Gonzalez, C.; Challacombe, M.; Gill, P. M. W.; Johnson, B.; Chen, W.; Wong, M. W.; Andres, J. L.; Gonzalez, C.; Head-Gordon, M.; Replogle, E. S.; Pople, J. A. *Gaussian 98*, revision A.11; Gaussian, Inc.: Pittsburgh, PA, 1998.

(23) (a) Perdew, J. P.; Wang, Y. *Phys. Rev. B* **1986**, *33*, 8800. (b) Perdew, J. P. *Phys. Rev. B* **1986**, *33*, 8822.

(24) Kutzelnigg, W.; Fleischer, U.; Schindler, M. *NMR−Basic Principles and Progress*; Springer: Berlin, Germany, 1990.

(25) (a) Salahub, D. R.; Fournier, R.; Mlynarski, P.; Papai, I.; St-Amant, A.; Ushio, J. In *Density Functional Methods in Chemistry*; Labanowski, J., Andzelm, J., Eds.; Springer: New York, 1991. (b) St-Amant, A.; Salahub, D. R. *Chem. Phys. Lett.* **1990**, *169*, 387. (c) Malkin, V. G.; Malkina, O. L.; Casida, M.; Salahub, D. R. *J. Am. Chem. Soc.* **1994**, *116*, 5898. (d) Malkin, V. G.; Malkina, O. L.; Eriksson, L. A.; Salahub, D. R. In *Modern Density Functional Theory: A Tool For Chemistry*; Seminario, J. M., Politzer, P., Eds.; Elsevier: Amsterdam, The Netherlands, 1995; Vol. 2. (e) Malkina, O. L.; Salahub, D. R.; Malkin, V. G. *J. Chem. Phys.* **1996**, *105*, 8793

(26) Dunning, T. H. *J. Chem. Phys.* **1987**, *98*, 1007.

(27) (a) Schreckenbach, G.; Ziegler, T. *J. Phys. Chem.* **1995**, *99*, 606. (b) Schreckenbach, G.; Ziegler, T. *Int. J. Quantum Chem.* **1997**, *61*, 899. (c) Wolff, S. K.; Ziegler, T. *J. Chem. Phys.* **1998**, *109*, 895. (d) Wolff, S. K.; Ziegler, T.; van Lenthe, E.; Baerends, E. J. *J. Chem. Phys.* **1999**, *110*, 7689.

(28) te Velde, G.; Bickelhaupt, F. M.; Baerends, E. J.; Fonseca Guerra, C.; van Gisbergen, S. J. A.; Snijders, J. G.; Ziegler, T. *J. Comput. Chem.* **2001**, *22*, 931. ADF 2002.01: http://www.scm.com.

(29) Becke, A. D. *Phys. Rev. A* **1988**, *38*, 3098.

(30) Marquez, B. L.; Gerwick, W. H.; Williamson, R. T. *Magn. Reson. Chem.* **2001**, *39*, 499.

(31) Tarpley, A. R.; Goldstein, J. H. *J. Mol. Spectrosc.* **1971**, *37*, 432.

(32) For the sake of clarity, we remark that the spin−orbit contribution that we refer to here means that coupling between the electron spin and the electron orbital momentum is included in the Hamiltonian. This is not to be confused with the spin−orbit contributions to the coupling constant (J^{DSO} and J^{PSO}), which are components of the coupling constant due to the coupling between the nuclear spin and the electron orbital momentum.

(33) Cheeseman, J. R.; Trucks, G. W.; Keith, T. A.; Frisch, M. J. *J. Chem. Phys.* **1996**, *104*, 5497.

(34) Noggle, J. H.; Schirmer, R. E. *The Nuclear Overhauser Effect−Chemical Applications*; Academic Press: New York, 1971.

(35) Quadrupolar relaxation takes place entirely through the modulation of the electric field gradient (efg) at the nucleus by molecular motions according to (for $I = {}^3/_2$) the following: $1/T_{2X} = \pi W_{1/2} = (2\pi^2/5)\chi^2[1 + (\eta^2/3)]\tau_c$, where χ is the nuclear quadrupolar coupling constant, η is its asymmetry parameter, and τ_c is the rotational correlation time. χ and η can be evaluated from calculated efg's at halogen nuclei. The efg tensor $\boldsymbol{q}$ can be expressed in terms of three principal components (q_{xx}, q_{yy}, q_{zz}, with axes defined so that q_{zz} is the largest), and the asymmetry parameter is given by $\eta = |q_{xx} - q_{yy}|/|q_{zz}|$. The nuclear quadrupolar coupling constant is $\chi = eQq_{zz}/h$, where Q is the nuclear quadrupole moment.[36] Efg components were obtained from the available relativistic spin−orbit density.[28] An accurate evaluation of T_{2X} is hampered by the uncertainty in τ_c; however, since the molecule is rigid it is reasonable to assume that the reorientation of q_{zz} for Cl and Br occurs with the same correlation time. Hence, the ratio of line widths is not affected by any particular such choice; the given values of T_{2X} were estimated assuming $\tau_c = 1$ ps. We also note that, as expected, scalar relaxation of the first kind (the frequency-independent term) is prevailing in the expression for $1/T_{2C}$, except for ^{79}Br where the two terms are comparable in magnitude.

(36) *CRC Handbook of Chemistry and Physics*; Lide, D. R., Ed.; CRC Press: Boca Raton, FL, 1997.

(37) Chertkov, V. A.; Sergeyev,N. M. *J. Am. Chem. Soc.* **1977**, *99*, 6750.